J. Am. Soc. Mass Spectrom. (2019) 30:2082–2091
DOI: 10.1007/s13361-019-02277-5

RESEARCH ARTICLE

Biomarker Mapping on Skin Tape Strips Using MALDI Mass Spectrometry Imaging

Guillaume Hochart,[1] David Bonnel,[1] Jonathan Stauber,[2] Georgios N. Stamatas[3]

[1]ImaBiotech SAS, 152 rue du Docteur Yersin, 59120, Loos, France
[2]ImaBiotech Corp, 44 Manning Road, Billerica, MA 01821, USA
[3]Johnson & Johnson Santé Beauté France, 1 rue Camille Desmoulins, 92130, Issy-les-Moulineaux, France

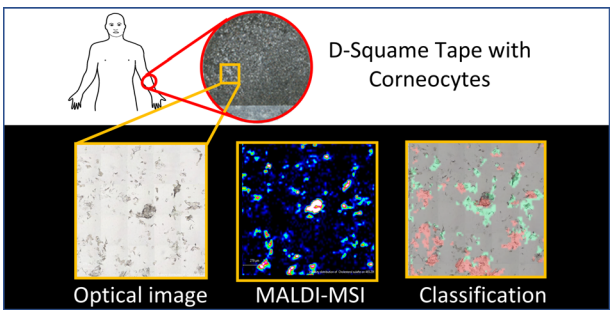

Abstract. Keratinocyte organization and biochemistry are important in forming the skin's protective barrier. Intrinsic and extrinsic factors can affect skin barrier function at the cellular and molecular levels. Matrix-assisted laser desorption/ionization (MALDI) mass spectrometric imaging, a technique which combines both molecular aspects and histological details, has proven to be a valuable method in various disciplines including pharmacology, dermatology and cosmetology. It typically requires ex vivo samples, prepared following frozen tissue sectioning. This paper demonstrates the feasibility of performing MALDI analysis on tape strips collected non-invasively on skin. The aim is to obtain molecular imaging of corneocytes on tapes towards novel biological insights. Tapes were collected from two skin sites (volar forearm and cheek) of human volunteers. Ten molecules relating to skin barrier function were detected with a single mode of acquisition at high spatial resolution with a 7 T MALDI-Fourier transform ion cyclotron resonance (FTICR) instrument. The method sensitivity was adequate to create molecular maps which could be overlaid on transmission microscopy images of the same area of the tape. Analysis of the molecular distributions from tapes at the two skin sites was consistent with the known skin properties of the two sites, confirming the validity of the observations. Hierarchical clustering analysis was used to differentiate corneocyte populations based on their molecular profiles. Furthermore, morphological analysis provided a new way of considering statistical populations of corneocytes on the same tape, rather than measuring a single averaged value, providing additional useful information relating to their structure-function relationship.

Keywords: Molecular mapping, Corneocytes, MALDI-FTICR mass spectrometry imaging, Skin barrier

Abbreviation AA Aminoacridine; ACN Acetonitrile; CHCA α-Cyano-4-hydroxycinnamic acid; DAN Diaminonaphtalene; DESI Desorption electrospray ionization; DHB Dihydroxybenzoic acid; FTICR Fourier transform ion cyclotron resonance; HD High definition; ITO Indium-tin-oxide; LC-MS/MS Liquid chromatography/mass spectrometry tandem; MALDI Matrix-assisted laser desorption/ionization; MS Mass spectrometry; MSI Mass spectrometry Imaging; NMF Natural moisturization factor; PCA Pyrrolidine carboxylic acid; RMS Root mean square; ROI Region of interest; TFA Trifluoroacetic acid; TOF-SIMS Time-of-flight secondary ion mass spectrometry; UCA Urocanic acid

Received: 16 October 2018/Revised: 13 June 2019/Accepted: 18 June 2019/Published Online: 12 August 2019

Introduction

The stratum corneum is the outermost layer of the skin constantly being exposed to the environment. Its function as a barrier is mainly conferred by the corneocytes, the terminal differentiated state of the epidermal keratinocytes, and their molecular interactions [1]. The barrier permeability can be

Electronic supplementary material The online version of this article (https://doi.org/10.1007/s13361-019-02277-5) contains supplementary material, which is available to authorized users.

Correspondence to: Guillaume Hochart;
e-mail: hochart.guillaume@imabiotech.com

modulated by intrinsic components (e.g., the presence of water solutes, such as the natural moisturizing factors) and lipids [2], as well as by various external factors.

Investigation of these phenomena is of high interest in dermatology and cosmetology, due to the ease of access with a topical treatment to repair or prevent alterations of this physical barrier. Intrinsic properties, such as skin aging, as well as external elements like the skin microbiome, are important areas of interest in this field.

The outermost most layer of the epidermis, the stratum corneum, is composed of dead cells (corneocytes) embedded in a lipid matrix. However, the stratum corneum is enzymatically very active and its activity relates to the condition of the skin, for example it can be altered with disease (e.g., eczema and psoriasis), with chronological age, with exposure to insults (pollution, UV, etc.), and with topical treatments [3]. Therefore, the study of the molecular environment of corneocytes is warranted.

Sampling of the stratum corneum can be performed by a simple, rapid, and non-invasive method using tape strips to collect surface corneocytes. The major advantage of this technique relies on the preservation of the spatial information [4]. Moreover, sequential tapes can be obtained at the same location to study consecutive cell layers of the stratum corneum only.

Besides nominal characterization of the intrinsic properties of the skin barrier, the clinical value of the tape sampling method is that the same site can be repeatedly sampled, for example before and after a treatment for comparison, with no or minimal damage to the tissue.

Post collection tape analysis requires adapted analytical tools to characterize the molecular environment of the corneocytes. Conventional mass spectrometry (MS) techniques, such as liquid chromatography (LC) MS/MS, are not suitable as they lose the spatial information.

To meet this requirement, analysis of corneocyte organization and biochemistry from skin tape strips has been described using different imaging techniques, each of them having its own advantages and drawbacks [5]. One way of acquiring molecular maps is through staining, for example using antibodies attached to a fluorophore or other specific chromo-reagents. The molecular information can be translated to useful physiological insights, for instance with the maturation state of the corneocytes [6]. In such methods, the number of detected molecules is limited to the number of stains that can be applied concurrently on the tape.

The nano-Time-of-Flight Secondary Ion Mass Spectrometry (TOF-SIMS) instrument provides cell imaging at submicron spatial resolution for the detection of small molecules only [7–11]. The desorption electrospray ionization (DESI)—mass spectrometry imaging (MSI) offers a broader mass range with a soft ionization technique, but with a lower spatial resolution, thus limiting the spatial information to arrive at histological details [5, 12].

Matrix-assisted laser desorption ionization (MALDI)—Fourier Transform Ion Cyclotron Resonance (FTICR) MSI is another technique that uses a laser with variable focus to achieve analysis at different spatial resolutions, down to 20 μm. It also allows to work on a broader mass range, from the metabolite to the protein level, with the benefit of providing the best mass accuracy compared with other mass spectrometry methods [13–19].

This paper describes the compatibility of the MALDI-FTICR MSI technique to detect different compounds related to the skin barrier function at high spatial resolution on human skin tape strips, collected at two different sites of the human body. The aim is to demonstrate not only the relevance of the molecular features from corneocytes, but also the ability to characterize their spatial distribution and structural features with accuracy.

A few challenges will be addressed, including the required sensitivity, the spatial resolution, and the ability to combine molecular images with high-definition light transmission microscopy images of the same areas. This feasibility study demonstrates the potential of this method in a variety of applications, some of which are described in this paper with preliminary data.

Experimental

Chemicals and Reagents

All chemicals, including 1,5-diaminonaphtalene (1,5-DAN), 9-aminoacridine (9-AA), 2,5-dihydroxybenzoic acid (DHB), α-cyano-4-hydroxycinnamic acid (CHCA), acetonitrile (ACN), LC-MS grade methanol, water, and trifluoroacetic acid (TFA), were purchased from Sigma-Aldrich (St. Louis, MO, USA). Indium-tin-oxide (ITO)-coated glass slides were purchased from Delta Technologies (Loveland, CO, USA). Sampling discs D-Squame were purchased from Cuderm Corporation (Dallas, Texas, USA).

Sample Collection, Tissue Preparation, and Technical Considerations

Sample Collection The study was conducted according to the Declaration of Helsinki and all human volunteers provided written informed consent. Skin tape strips were collected from two volunteers at two different collection sites: volar forearm and cheek. The volunteers were instructed not to apply any skin care product for at least 24 h before the experiment. The tapes were applied on the skin site of interest using gentle pressure and were removed after 30 s using forceps. Two consecutive tapes were applied on the same site. The first tape was discarded to remove any skin surface contamination from external factors. The second tape was placed in a scintillation vial and the vial was placed on dry ice and later stored at − 20 °C until further use. The process was repeated at the next skin area. Each body site (face or forearm) was sampled three times at neighboring areas. Each stored tape was named according to the following VSN code (Supplementary material Figure 1a):

V volunteer (1 or 2);
S site (1 for arm, 2 for face);
N sequential number

High-definition Light Transmission Microscopy of the Skin Tapes HD optical scans were performed at zoom × 20 with the Scanner HD Pannoramic 250 Flash 2 (3DHISTECH, Budapest, Hungary) prior to matrix deposit.

Tissue Mounting Strips were collected after drying by pairs consisting of one skin tape from the arm and one skin tape strip from the cheek of the same volunteer per slide. Red marks were done on the non-adhesive face of strips to visualize acquisition areas.

Strip pairs were fixed using adhesive tape (3 M XYZ-Axis Electrically Conductive Tape 9713, 3 M, Cergy, France) on Superfrost slides, adhesive face of strip facing up. The Superfrost slide was then scanned at × 20 with the Pannoramic 250 Flash 2..

After scanning, tape strips (control and skin) were removed from the Superfrost slide and fixed on an indium-tin-oxide slide covered with conductive tape.

A negative control consisting of a quarter tape strip free from skin was added (Supplementary material Figure 1b, c).

MALDI Matrix Deposit MALDI matrices 2,5-dihydroxybenzoic acid (DHB) at 40 mg/mL in 1:1 methanol:0.1% trifluoroacetic acid (TFA) *v*/*v* and α-cyano-4-hydroxycinnamic acid (CHCA) at 10 mg/mL in 6:4 ACN:0.1% TFA *v*/*v* for the positive ionization mode, and 1,5-diaminonaphtalene (DAN) at 10 mg/mL in 1:1 methanol:water *v*/*v* and 9 amino-acridine (9-AA) at 10 mg/mL in 4:1 methanol:water *v*/*v* for the negative ionization mode were sprayed on the tape strips with the automatic TM Sprayer device (HTX Imaging, Chapel Hill, NC, USA). For the DAN matrix, settings of the TM sprayer were 100 µL/min as a flow rate, 60 °C for the nozzle temperature, 2 L/min for the gas, 10 layers (respectively around 20 mg and 3 mg matrix deposits for DHB and DAN).

Targeted Molecules and Analysis by MALDI-FTICR Mass Spectrometry

MALDI MSI was performed at high spatial resolution (20 µm) using a 7 T-MALDI-FTICR (SolariX, Bruker Daltonics, Bremen, Germany) with a Smartbeam II laser in minimum mode and a repetition rate at 2000 Hz.

Full scan positive mode in 75–600 Da mass range was selected for the imaging of regions of interest (ROI) of around 5 mm^2 per tape strip with online calibration using MALDI matrix peaks. Mass accuracy was under 1 ppm for the targeted ions. The mass spectrum obtained for each position of the images corresponds to the averaged mass spectra of 200 consecutive laser shots on the same location. FTMS control 2.1.0 and FlexImaging 4.1 software packages (Bruker Daltonics, Bremen, Germany) were used to control the mass spectrometer and set imaging parameters.

The different MALDI matrices were investigated according to the expected ionization of targeted molecules (lipids, amino acids and metabolites) in the pre-screening test, before focusing on ten targeted molecules with a single mode of acquisition (negative ionization).

Data Analysis

Bruker software suite including suite FTMS control 2.1.0, FlexImaging 4.1, and DataAnalysis 4.2 were used for recording the data and previsualization of the data.

Data treatment, optical and molecular images were processed with Multimaging 1.1 software (ImaBiotech SAS, Loos, France) and ImageJ (U. S. National Institutes of Health, Bethesda, MD, USA).

Results

MALDI-FTICR Technical Approach

Characterization of the MS Signal of Target Biomolecules This preliminary phase aimed at evaluating the detection of specific compounds meaning that no molecular species from the tape support or the matrix (or combination of both) should interfere with the molecular features from the keratinocytes. It was also meant to test the MALDI laser in minimum mode to achieve the required 20-µm spatial resolution, which would allow us to detect the molecular signals from the corneocytes with adequate sensitivity.

In positive mode of ionization, the CHCA and DHB matrices allowed only the detection of L-arginine and histidine on the skin tape strips. However, using the CHCA matrix, interfering signals were also detected in the control tape strip and only arginine could be discriminated as sodium or potassium adduct, since the protonated form was mixed with an interfering peak from the tape. DHB allowed the same detection with the advantage of no interfering peak from the tape.

Table 1. Detection of Targeted Molecules in Positive (DHB matrix) and Negative (DAN matrix) Modes of Ionization. x, Detected; −, Not Detected; *ta*, Tape Adhesive Interferent; *m*, Matrix Interferent

Name	Formula	Positive mode	Negative mode
C16:1	C16H30O2	–	x (ta)
C16:0	C16H32O2	–	x (m)
C18:1	C18H34O2	–	x (ta)
C24:0	C24H48O2	–	x
C26:0	C26H52O2	–	x
Sphingosine*	C18H37NO2	–	–
Glycerol*	C3H8O3	–	–
Cholesterol sulfate	C27H46SO4	–	x
Squalene*	C30H50	–	–
Cholesterol*	C27H48O	–	–
D/L-Arginine	C6H14N4O2	x	x
Lactic acid*	C3H6O3	–	–
D/L-Histidine	C6H9N3O2	x	x
Urea*	CH4N2O	–	–
Urocanic acid	C6H6N2O2	–	x
Pyrrolidine carboxylic acid	C5H7NO3	–	x

*Not selected for the imaging

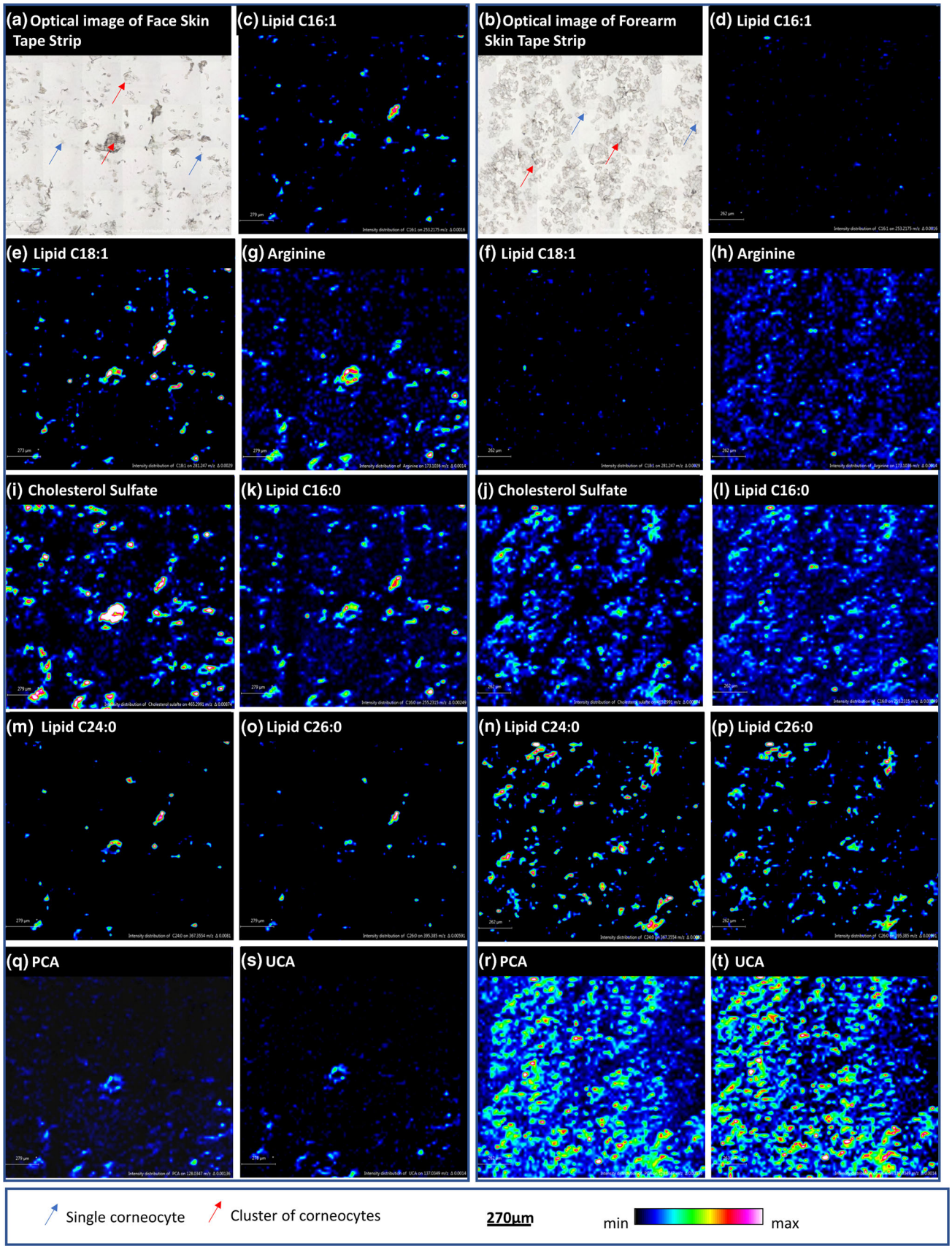

Figure 1. Optical images (**a**, **b**) and comparison of molecular distributions of C16:1 (*m/z* 253.22) (**c**, **d**), C18:1 (*m/z* 281.25) (**e**, **f**), arginine (*m/z* 173.10) (**g**, **h**), cholesterol sulfate (*m/z* 465.30) (**i**, **j**), C16:0 (*m/z* 255.23) (**k**, **l**), C24:0 (*m/z* 267.35) (**m**, **n**), C26:0 (*m/z* 395.38) (**o**, **p**), PCA (*m/z* 128.03) (**q**, **r**), and UCA (*m/z* 137.03) (**s**, **t**) between face skin tape strip and forearm skin tape strip

As expected from the chemical structures of most of the compounds, the DAN matrix for the negative mode showed very promising results as it allowed the detection of ten compounds of interest including arginine and histidine. Interfering species either from the matrix or the adhesive were detected for the C16:1, C16:0, and C18:1 lipids, but with low intensity compared with the signal from the corneocytes.

Following the results of good detection of multiple molecules of interest, the DAN matrix was selected for the imaging of the keratinocytes on skin tape strips for 10 selected compounds (Table 1).

Overlay of Optical Image and Molecular Image at High Spatial Resolution We attempted to combine the molecular maps provided by the MALDI-FTICR method with topological details of the spatial distribution of the corneocytes. To achieve this goal, the molecular map at highest spatial resolution (20 µm) was overlaid over the digitalized optical image provided by the HD scanner.

Distribution Results

The color map look-up tables representing the intensity scales of the molecular signals were adjusted for each MALDI image to reduce the noise for better visualization of the signal across the tapes. Because of this, for compounds having signals close to the noise level, particularly lipids C16:1 and C18:1, only the highest signals were visualized (Figure 1a–f).

The intensity scale for lipid C16:0 was not adjusted, because of the low signal level. However, the molecular signal coming from the corneocytes can be distinguished in certain regions in Figure 2.

The endogenous compounds C16:1, C18:1, arginine, and cholesterol sulfate (Figure 1c–j) are more likely to be detected on the sample from the cheek site.

The facial skin is characterized by higher activity of the sebaceous glands compared with the volar forearm [20]. This may explain the higher intensities of mono-saturated free fatty acids C16:1 and C18:1 and cholesterol sulfate in Figure 1, which are certainly correlated with higher concentrations.

The endogenous compounds C16:0, C24:0, C26:0, pyrrolidine carboxylic acid (PCA), and urocanic acid (UCA) are more likely to be detected in the forearm skin strip (Figure 1k–t).

The lower production of sebum on the volar forearm site may explain the presence of long saturated fatty acids at higher concentrations [21]. Also, the lower cell turnover rates on the arm compared with the face [22, 23] translate into longer transition times for filaggrin-related proteins

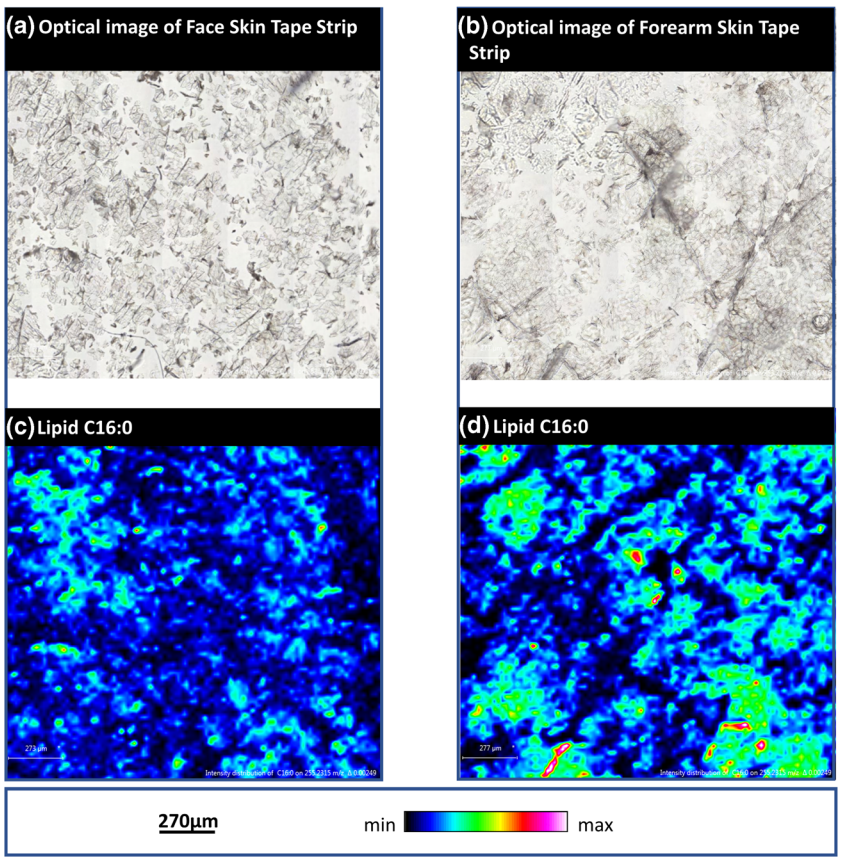

Figure 2. Optical images (**a**, **b**) and comparison of molecular distributions of C16:0 (*m/z* 255.23) (**c**, **d**) between face skin tape strip and forearm skin tape strip

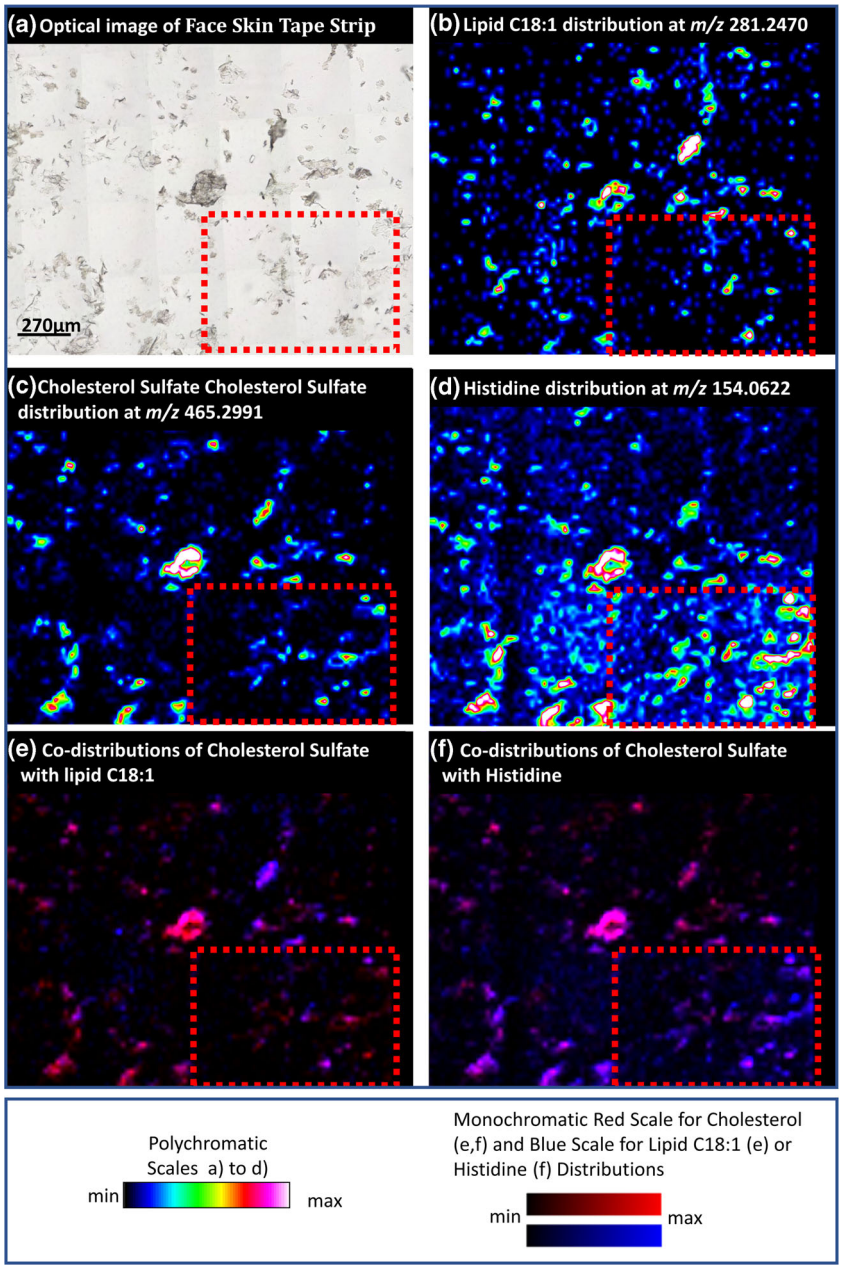

Figure 3. Optical images of face skin tape strip (**a**) and molecular images of lipid C18:1 (*m/z* 281.25) (**b**), cholesterol sulfate (*m/z* 465.30) (**c**), and histidine (*m/z* 154.06) (**d**) with polychromatic scale; co-distributions of cholesterol sulfate with lipid C18:1 (**e**) or with histidine (**f**)

that are hydrolyzed in the stratum corneum to give rise to components of the natural moisturization factor (NMF), such as PCA and UCA. In contrast, due to the high cell turnover rates on the cheek, there is not enough time for full enzymatic degradation of filaggrin, which translates into lower amounts of NMF [24].

The distribution of histidine between the two body sites appears to be equal (data not shown). This finding may indicate that there may be other sources of histidine (and arginine), besides the degradation of filaggrin and similar molecules of the S100 family of proteins [25].

Discussion

Sample Cohort

This study was designed to test the feasibility of using MALDI MSI on skin tape strips. We tested this hypothesis on tapes collected from two skin locations (face and arm) and compared the relative abundance and spatial distribution of biomolecules that play key role in the formation of the skin barrier. We demonstrated in a small sample that there are differences between the distributions and the relative abundances of the molecules of interest between the two sites. A physiological

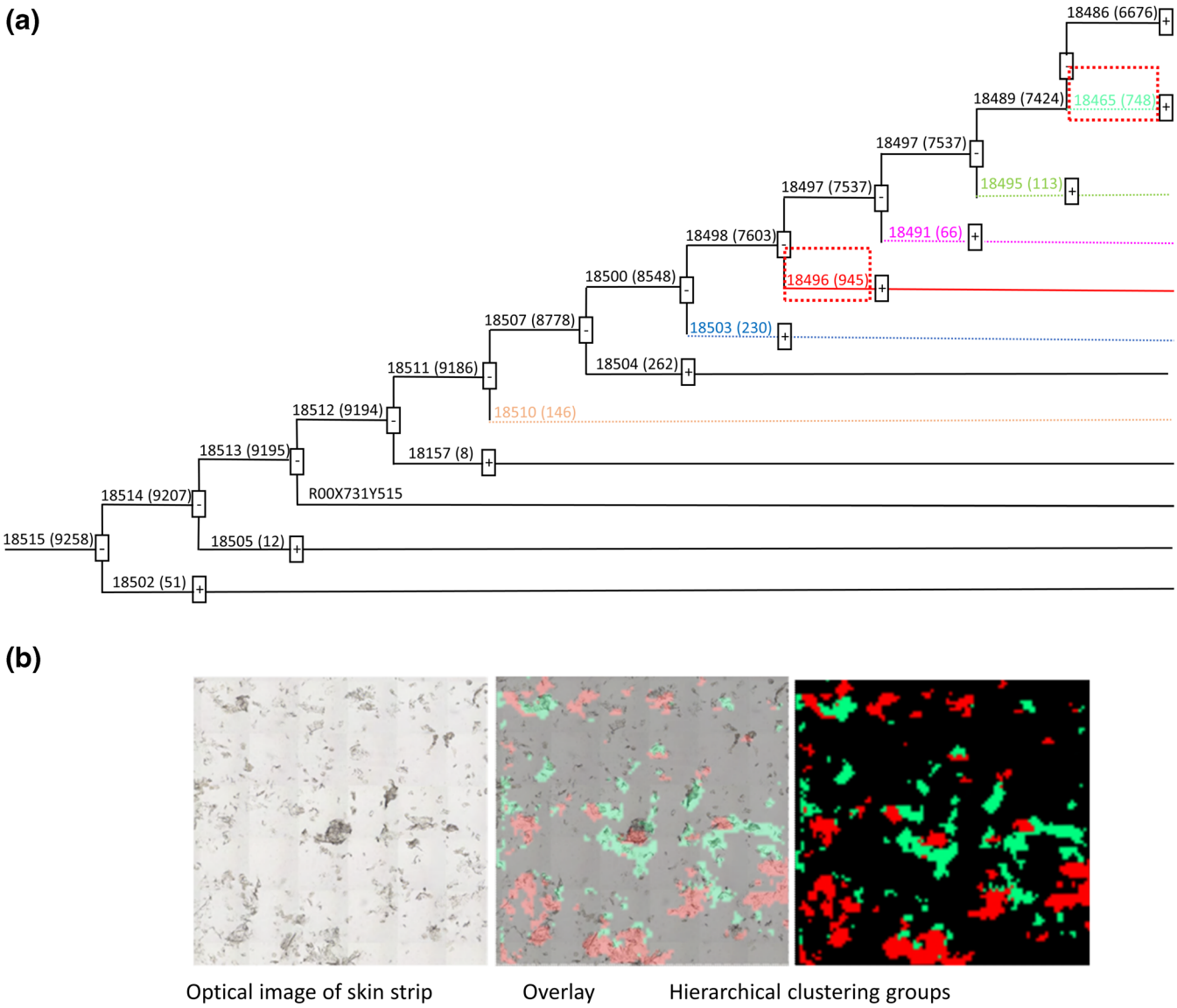

Figure 4. Hierarchical clustering in face skin tape strip (**a**) dendrogram; (**b**) illustration of two classes of corneocytes (dash-squared areas) based on their molecular profiles

base for such differences can be hypothesized, but larger cohort studies are needed to confirm.

Molecular Abundance Mapping Overlay

Comparing the distribution and relative abundance of different molecules on the same tape revealed differences among the targeted ions.

This was particularly observed in clusters of corneocytes, where the 20-µm spatial resolution was able to visualize differences for example in comparing two lipids, a lipid with a metabolite or a lipid with an amino-acid, as demonstrated in Figure 3. Cholesterol sulfate and the monounsaturated lipid C18:1 distributions were found to be heterogenous (Figure 3b, c), particularly on the cluster of corneocytes (towards the center of the image). They were preferentially found in areas appearing darker in the optical image, relating to more densely populated regions. However, histidine (Figure 3d) was found more evenly distributed between corneocytes as shown in the red square region (relatively isolated corneocytes) for which lipid C18:1 and cholesterol sulfate are poorly present.

This was further demonstrated by overlaying the molecular maps, where the molecular abundances are represented by different colors for each molecule (Figure 3e, f).

These results indicate that on a single tape there are populations of corneocytes having varied molecular profiles and likely varied contributions to the physicochemical properties of the skin.

Another way to visualize such compositional differences between corneocyte populations on the same tape is to calculate ratios of the relative abundances of two biomolecules.

It should be noted that normalization by the root mean square (RMS) algorithm was checked in the data in Fleximaging software to verify the trend of molecular

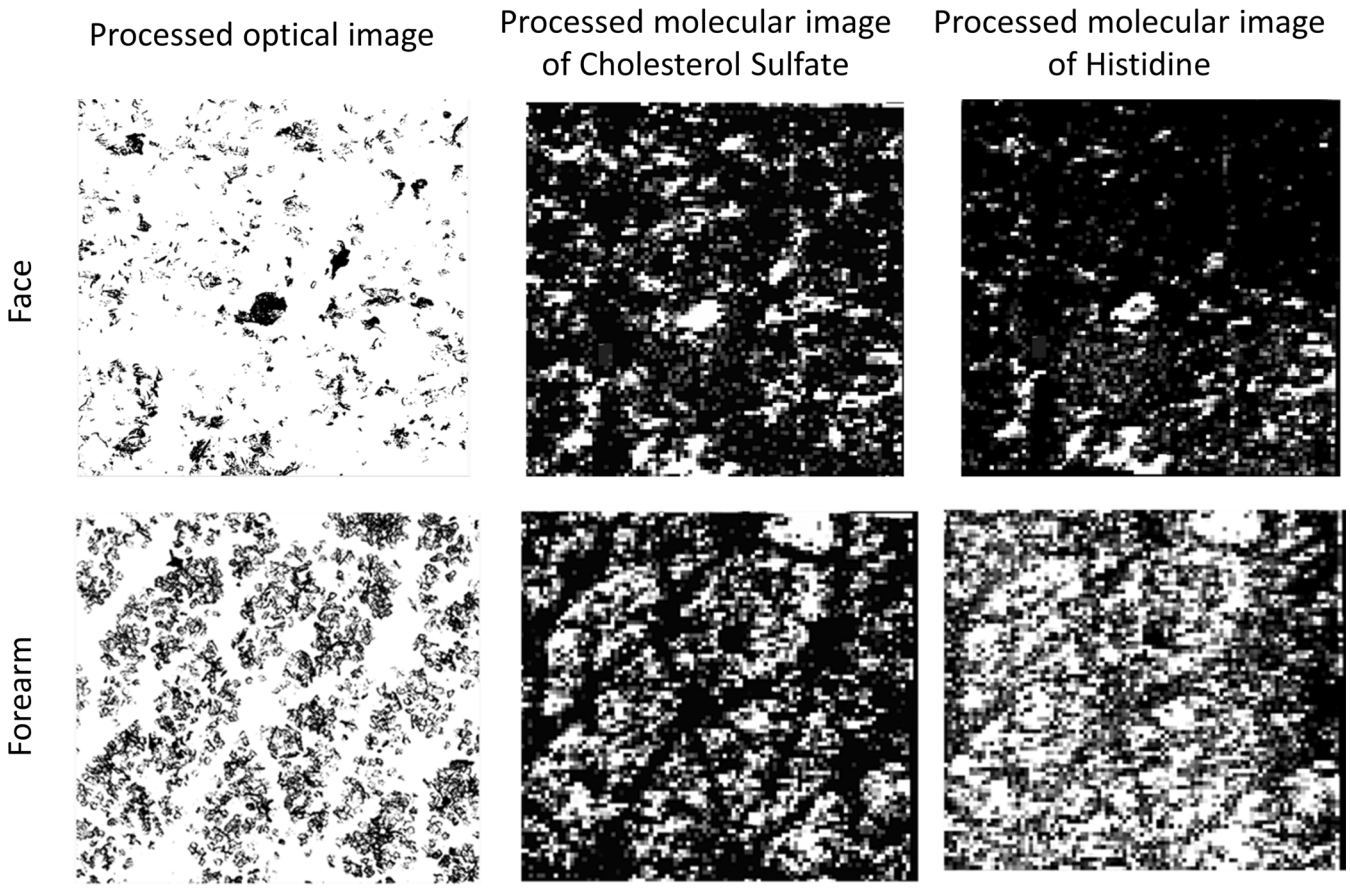

Figure 5. Binarization of optical and molecular images (no convolution applied) for morphological approach. White color illustrates the distribution of the compounds

responses with respect to the potential extinction effects relating to corneocytes or the adhesive from the tape. To refine the accuracy of the data normalization regarding these extinction effects, a specific stable labeled isotope should be used per compound of interest since they may have different ionization responses.

The feasibility of performing MALDI MSI on skin tapes demonstrates the possibility to assign endogenous or exogenous molecular signals to topological details at the corneocyte level. Furthermore, this method opens the prospect of studying the effects of body location, skin phenotype, aging, environmental stressors, skin microbiome, etc. on the biochemical composition of corneocytes.

Classification

Different approaches can be used to compare tape strips depending on morphologic (size of cell cluster, number of cells per cluster, etc.) and compositional parameters.

Hierarchical Clustering/Principal Component Analysis A classification algorithm, known as hierarchical clustering based

Table 2. Evaluation of Molecular Coverage (%) of Corneocyte Contribution (empty spaces excluded)*, Based on Intensity Scales Selected for the Comparison with the Background of Adhesive Tape Only (no tissue effect considered)

	Cholesterol sulfate image		Histidine image	
Skin site	Forearm	Face	Forearm	Face
Sample ID	214	224	214	224
Number of objects*	288	167	351	144
Surface objects (pixels)*	629,117	252,228	630,647	176,457
Total surface (pixels)	2,662,065	2,530,881	2,662,065	2,530,881
Surface objects optical (pixels)	581,241	228,461	581,241	228,461
Coverage (%)	23.6	10.0	23.7	7.0
Coverage molecular/optical (%)	108.2	110.4	108.5	77.2

on similarities in the molecular profiles, could be used to classify the corneocytes on the skin tapes. This approach was assessed to visualize two distinct classes of corneocytes, consisting respectively of 945 and 748 spectra having their own specific molecular profile (Figure 4).

The compositionally distinct classes of corneocytes may correspond to subpopulations for example of cells at different maturation stage, defined by the relative abundance of lipids and involucrin, as has been demonstrated before by staining techniques [6].

An alternative and complementary approach would consist of running a principal component analysis on pre-established classes of corneocytes or on the entire sample, to define specific molecular profiles between corneocytes.

Morphometric Approach Briefly, this approach would allow the identification of differences between tapes, by taking into account the morphological parameters of the clusters, their size and shape at each molecular mapping. It can also be used to calculate the signal intensity corresponding to targeted species per cluster, averaged over the surface area of the cluster, beyond just averaging over the whole ROI area [26]. The samples consist of isolated corneocytes or clusters of corneocytes with empty spaces in-between (tape only). Such empty regions should be excluded during averaging. This was achieved by binarizing the image as illustrated in Figure 5.

The optical image and the molecular distribution of cholesterol sulfate and histidine are both binarized. The number of objects, defined as non-background connected groups of pixels [9], was then calculated for each image, before evaluating the coverage of molecular signal in the keratinocytes.

The results indicated that the two targeted ions covered almost all the corneocytes (Table 2) except for histidine in the cheek sample with 77% of coverage. It is possible that this relates to the slow cell turnover rate on the face.

A similar approach could be extended to different samples from the same individual to compare skin layers of one or several sites of collection or from different individuals to correlate targeted ions with corneocyte size and shape.

In this paper, we demonstrated that MALDI-MSI can be very useful as an investigative method combined with skin surface tape stripping. Distribution maps of selected molecules can be constructed and their relative concentrations can be assigned to corneocytes or clusters of corneocytes with a single mode of acquisition. The results revealed differences between the samples from the face and the forearm site that are pointing to relevant physiological differences. This information can be used to characterize intrinsic skin properties, as well as applied to research relating to skin microbiome, skin disease, and effects of topical formulations.

Acknowledgements

The authors would like to thank Gaël Picard de Müller and Fabien Pamelard for their contribution to the morphologic and statistical approaches.

Compliance with Ethical Standards

Conflict of Interest GNS is employee of Johnson & Johnson Santé Beauté France, a manufacturer of skin care products. GH, DB, and JS are employees of ImaBiotech, SAS a provider of analytical services including MALDI-MSI. The authors of the manuscript declare no competing commercial/financial interests.

References

1. Proksch, E., Brandner, J.M., Jensen, J.-M.: The skin: an indispensable barrier. Exp. Dermatol. **17**, 1063–1072 (2008)
2. Sakai, S., Sasai, S., Endo, Y., Matue, K., Tagami, H., Inoue, S.: Characterization of the physical properties of the stratum corneum by a new tactile sensor. Skin Res. Technol. **6**, 128–134 (2000)
3. Rawlings, A.V.: Recent advances in skin "barrier" research. J. Pharm. Pharmacol. **62**, 671–677 (2010)
4. Pierard, G.E.: EEMCO guidance for the assessment of dry skin (xerosis) and ichthyosis: evaluation by stratum corneum shippings. Skin Res. Technol. **2**, 3–11 (1996)
5. Hendrix, S.W., Miller, K.H., Youket, T.E., Adam, R., O'Connor, R.J., Morel, J.G., Tepper, B.E.: Optimization of the skin multiple analyte profile bioanalytical method for determination of skin biomarkers from D-Squame tape samples. Skin Res. Technol. **13**, 330–342 (2007)
6. Hirao, T., Denda, M., Takahashi, M.: Identification of immature cornified envelopes in the barrier-impaired epidermis by characterization of their hydrophobicity and antigenicities of the components. Exp. Dermatol. **10**, 35–44 (2001)
7. Kezutyte, T., Desbenoit, N., Brunelle, A., Briedis, V.: Studying the penetration of fatty acids into human skin by ex vivo TOF-SIMS imaging. Biointerphases. **8**, 3 (2013)
8. Cizinauskas, V., Elie, N., Brunelle, A., Briedis, V.: Fatty acids penetration into human skin ex vivo: a TOF-SIMS analysis approach. Biointerphases. **12**, 11003 (2017)
9. Sjovall, P., Greve, T.M., Clausen, S.K., Moller, K., Eirefelt, S., Johansson, B., Nielsen, K.T.: Imaging of distribution of topically applied drug molecules in mouse skin by combination of time-of-flight secondary ion mass spectrometry and scanning electron microscopy. Anal. Chem. **86**, 3443–3452 (2014)
10. Sjovall, P., Skedung, L., Gregoire, S., Biganska, O., Clement, F., Luengo, G.S.: Imaging the distribution of skin lipids and topically applied compounds in human skin using mass spectrometry. Sci. Rep. **8**, 16683 (2018)
11. Siekkeri Vandikas, M., Hellstrom, E., Malmberg, P., Osmancevic, A.: Imaging of vitamin D in psoriatic skin using time-of-flight secondary ion mass spectrometry (ToF-SIMS): a pilot case study. J. Steroid Biochem. Mol. Biol. **189**, 154–160 (2019)
12. D'Alvise, J., Mortensen, R., Hansen, S.H., Janfelt, C.: Detection of follicular transport of lidocaine and metabolism in adipose tissue in pig ear skin by DESI mass spectrometry imaging. Anal. Bioanal. Chem. **406**, 3735–3742 (2014)
13. Caldwell, R.L., Caprioli, R.M.: Tissue profiling by mass spectrometry: a review of methodology and applications. Mol. Cell. Proteomics. **4**, 394–401 (2005)
14. Cornett, D., Frappier, S., Caprioli, R.: MALDI-FTICR imaging mass spectrometry of drugs and metabolites in tissue. Anal. Chem. **80**, 5648–5653 (2008)
15. Bonnel, D., Legouffe, R., Eriksson, A.H., Mortensen, R.W., Pamelard, F., Stauber, J., Nielsen, K.T.: MALDI imaging facilitates new topical drug development process by determining quantitative skin distribution profiles. Anal. Bioanal. Chem. (2018). https://doi.org/10.1007/s00216-018-0964-3
16. Lewis, E.E.L., Barrett, M.R.T., Freeman-Parry, L., Bojar, R.A., Clench, M.R.: Examination of the skin barrier repair/wound healing process using a living skin equivalent model and matrix-assisted laser desorption-ionization-mass spectrometry imaging. Int. J. Cosmet. Sci. **40**, 148–156 (2018)

17. Russo, C., Brickelbank, N., Duckett, C., Mellor, S., Rumbelow, S., Clench, M.R.: Quantitative investigation of terbinafine hydrochloride absorption into a living skin equivalent model by MALDI-MSI. Anal. Chem. **90**, 10031–10038 (2018)
18. Sorensen, I.S., Janfelt, C., Nielsen, M.M.B., Mortensen, R.W., Knudsen, N.O., Eriksson, A.H., Pedersen, A.J., Nielsen, K.T.: Combination of MALDI-MSI and cassette dosing for evaluation of drug distribution in human skin explant. Anal. Bioanal. Chem. **409**, 4993–5005 (2017)
19. Nguyen, J., Lewis, H., Queja, A., Diep, A.N., Hochart, G., Ameri, M.: Pharmacokinetics and skin tolerability of intracutaneous zolmitriptan delivery in swine using adhesive dermally applied microarray. J. Pharm. Sci. **107**, 2192–2197 (2018)
20. Marrakchi, S., Maibach, H.I.: Biophysical parameters of skin: map of human face, regional, and age-related differences. Contact Dermatitis. **57**, 28–34 (2007)
21. Firooz, A., Sadr, B., Babakoohi, S., Sarraf-Yazdy, M., Fanian, F., Kazerouni-Timsar, A., Nassiri-Kashani, M., Naghizadeh, M.M., Dowlati, Y.: Variation of biophysical parameters of the skin with age, gender, and body region. ScientificWorldJournal. **2012**, 386936 (2012)
22. Hayashi, S., Matsue, K., Takiwaki, H.: Image analysis of the distribution of turnover rate in the stratum corneum. Skin Res. Technol. **4**, 109–120 (1998)
23. Kashibuchi, N., Hirai, Y., O'Goshi, K., Tagami, H.: Three-dimensional analyses of individual corneocytes with atomic force microscope: morphological changes related to age, location and to the pathologic skin conditions. Skin Res. Technol. **8**, 203–211 (2002)
24. Rawlings, A.V., Harding, C.R.: Moisturization and skin barrier function. Dermatol. Ther. **17**(Suppl 1), 43–48 (2004)
25. Wu, Z., Hansmann, B., Meyer-Hoffert, U., Gläser, R., Schröder, J.-M.: Molecular identification and expression analysis of filaggrin-2, a member of the S100 fused-type protein family. PLoS One. **4**, e5227 (2009)
26. Picard de Muller, G., Ait-Belkacem, R., Bonnel, D., Longuespee, R., Stauber, J.: Automated morphological and morphometric analysis of mass spectrometry imaging data: application to biomarker discovery. J. Am. Soc. Mass Spectrom. **28**, 2635–2645 (2017)